FINITE ELEMENT ANALYSIS OF SUPERPLASTIC FORMING PROCESS USING LS-DYNA

Authors:

Haryanti Samekto [a]

Karl Roll [b]

[a]PhD Student,
Institut Fuer Umformtechnik
Universitaet Stuttgart, Stuttgart, Germany

[b]Professor,
DaimlerChrysler AG Werk Sindelfingen,
Sindelfingen, Germany

Correspondence:

Haryanti Samekto
Institut Fuer Umformtechnik
Holzgartenstrasse 17
D-70174 Stuttgart
Germany

Tel: +49-(0)711-1212303
Fax: +49-(0)0711-1212309
e-mail: haryanti@ifu.uni-stuttgart.de

Abstract

Superplastic forming process has been a standard manufacturing process in aircraft industry and its applications in other industries are increasing. Superplasticity is utilised in forming parts which can not be produced technically or economically using materials with ordinary ductility. As superplastic deformation should be carried out under certain strain rate in which m value is maximal, the finite element method is applied to model the forming process in order to optimise the process through generating a pressure-time curve. In this paper, the dynamic explicit solution procedure was taken as an alternative solution due to its efficiency, as most of the current simulations of SPF used static implicit. The material parameters of Aluminium alloy 5083 SPF were first determined and the creep constitutive model was chosen. The finite element analysis results from dynamic explicit were verified with experimental results and then compared with static implicit. The simulation of bulge forming process with the geometry of a cup was conducted. The effects of m value and friction coefficient value were investigated.

Keywords: Superplastic foming, Finite element, aluminium 5083

1   Introduction

Under certain conditions, certain metallic alloys and ceramics exhibit a phenomenon called superplasticity, in which these materials manage to undergo an elongation more than 100% without rupture. Even, an elongation of about 5000 % has been obtained by Higashi [1] in aluminium bronze. Superplastic forming technique is applied to form parts with complex geometries which can not be easily produced by materials with limited ductility. The main purpose of developing superplastic forming (SPF) is to achieve near-net shape process and to obtain single-piece components. This is considerably saving in material cost and in labour intensive machining cost such as: tooling, finishing and joining, as well as reducing the weight and increasing the strength of the product.
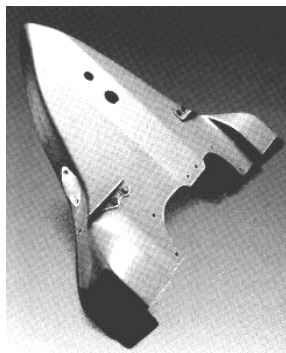
a. Aircraft: F-18 bomb rack   b. Automotive: door panel

Fig. 1. Parts produced by superplastic forming process [2]

The main requirements of superplasticity are: First is the micrograin structure. The material has to have a very fine and stable grain size (less than 10 μ). Second, the temperature of the process has to be elevated about half of the melting point. Third, the process has to be carried out in a low and controlled strain rate, usually 10^{-4} to 10^{-2} per second. Due to the requirements above, only limited number of alloys can be applied in SPF. Aluminium is one of the most potential materials in SPF.

Aluminium-Magnesium alloy 5083 is inexpensive alloy and it has good weldability, good corrosion resistance and moderate strength. Superplastic sheet of Al 5083 can be produced from commercial 5083 alloy by modifying chemical composition, such as addition of Cu or Zr which function as grain refiner, and then thermomechanical treatment as a following process. Hot cross rolling will prevent the grain growth in a certain direction. As a result equiaxed grains will be obtained. This superplastic alloy is attractive for the application in automotive industry, in which the requirements of materials properties are not as high as aircraft industry.

Many numerical analysis have been conducted to optimise the process. Non-finite element analysis of SPF is usually confined to the simple geometries, and to enable carrying out the analysis, some behaviour of the forming sheet are simplified [3, 4, 5, 6]. These simplifications are not required in finite element analysis. In general, finite element analysis is able to provide more information about the process parameters than non-finite element analysis. The non-finite element analysis is effective only to gain an insight of the simple changing of the process parameters. Whereas, finite element analysis can provide these factors such as: the complexity of the geometry, die's parameters, the pressure cycle, un-uniformity of the blank, friction conditions and microstructural changes can be included.

2   Material Constitutive Model

Many factors have to be considered in determining a valid constitutive material of a superplastic material, namely: grain size, strain, temperature and the density of cavitations. However, if mechanical aspects are considered, superplastic deformation shows similarities with creep deformation stage II, or stationary creep, in which the slope of the curve is constant. The presence of steady state in the stationary creep curve, in which the strain rate is constant at a given stress, can be compared with superplastic flow [7].

The simple constitutive equation, which is used for standard metalworking, is:

$$\overline{\sigma} = K\varepsilon^{n}\dot{\varepsilon}^{m} \qquad\qquad (1)$$

In which $\overline{\sigma}$ is the flow stress, K is a material constant, ε is the strain, n is the strain hardening exponent, $\dot{\varepsilon}$ is the strain rate and m is the strain rate sensitivity index. The values of K, m and n can be easily estimated by using regression analysis.

3   Determination of the Material Parameters

Material for this study was Aluminium alloy 5083 with a brand name FORMALL 545 produced by Alusuisse. This commercial alloy had been manufactured specially for superplastic forming applications and delivered as rolled sheet of 1.6 mm thick.

a. Geometry of the Specimen

b. Specimens after test
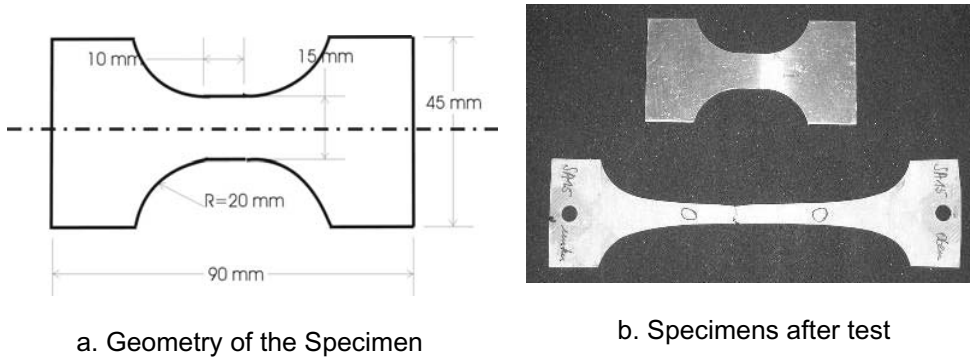
Fig. 2. Tensile test specimen

3.1   Determination of m Value

As mentioned above that superplasticity stipulates a low and constant strain rate, therefore instead of constant cross head velocity, the tensile tests were carried out in constant strain rates. The crosshead velocity was changed continuously according to the change of the specimen lenght by using the expression below:

$$V = \dot{\varepsilon}\, l_0 \exp(\dot{\varepsilon}\, t) \tag{2}$$

Where V is the crosshead velocity, l_0 is the initial gauge length and t is the time of the conducting test.

Neglecting the strain hardening, we could simplify modify equation (1) into:

$$\sigma = K\,\dot{\varepsilon}^{\,m} \tag{3}$$

If a curve is generated with co-ordinates $\log\sigma$ and $\log\dot{\varepsilon}$, a linear relationship can be obtained. The slope of the linear line is equal to m. However, experimental data could not be conventionally fitted by such a linear line, typically a sigmoidal curve was produced, as shown in Fig. 1. It is often said in many literatures that equation (1) should to be treated as a local approximation of the sigmoidal plot, which is valid within a sufficiently narrow strain rate interval, where the hypothesis m value is constant can be adopted with a reasonable accuracy. Considering that a linear relationship between $\log\sigma$ and $\log\dot{\varepsilon}$ is only valid in a narrow range, another approach of strain rate sensitivity was developed.

$$m = \frac{\partial \ln\sigma}{\partial \ln\dot{\varepsilon}} \tag{4}$$

The expression above shows that the value of m is not uniform, but it is a function of strain rate. Backofen [8] introduced a velocity jump test in which a tensile specimen is deformed at a constant velocity until a steady state is reached, and the velocity is then increased.

Due to the decreasing strain rate during the tensile test, a jumping strain rate rather than jumping velocity is preferred if the strain rate can be maintained constant [9, 10]. This method was applied in this paper.

Fig. 3 shows the true stress - true strain curve for a jump strain rate from expected constant strain rate from 1.10^{-3}/s to 1.10^{-2}/s. Fig. 5 shows the plot of true strain profile. From those results, the m value could be determined:

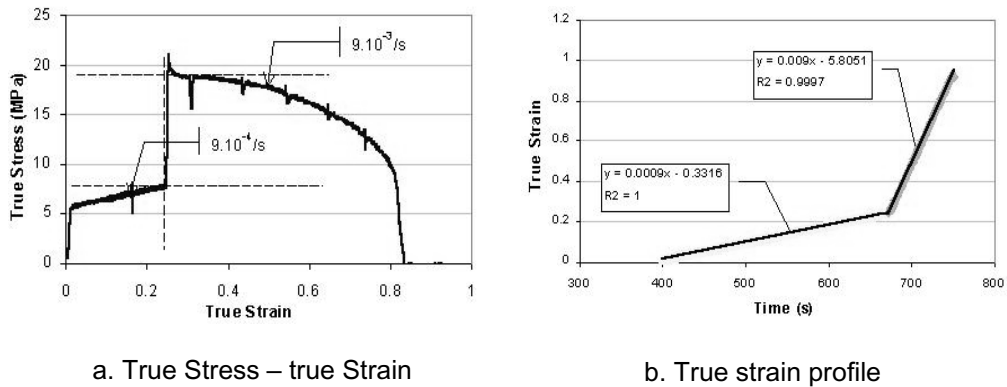|	
a. True Stress – true Strain	b. True strain profile

Fig. 3. Stress and strain plots for jump strain rate

Calculation was carried out for other jumping strain rates in order to find out the value of the strain rate sensitivity for every strain rate. The result presents in Fig. 4. It was very typical for superplastic material that the m value was maximum in certain range. As the higher m value provided the better resistance to material instability, therefore the strain rate in a superplastic forming process should be maintained in the range in which the m value is maximum. The maximum value 0.53 was reached at strain rate 1.10^{-4}/s in this jump strain rate method.
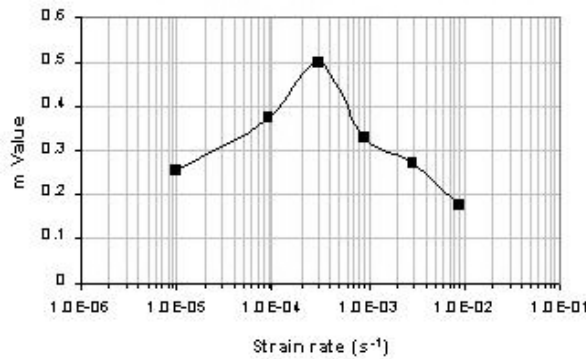
Fig. 4. The value of strain rate sensitivity for different strain rates

3.2   Material Parameter Input

The constitutive material available in LS-DYNA which can accommodate superplastic behaviour most likely was the material number 64 MAT RATE SENSITIVE POWER LAW PLASTICITY. As superplastic deformation was dominated by large plastic deformation, the elastic deformation was neglected. Strain hardening was ignored by giving a very low value of n, even n = 0 could be used. The large deformation in superplasticity occurred in the area after uniform elongation. Therefore, the flow stress was affected only by the strain rate. The detailed value of each parameters were given as follows:

Parameter	Value	Unit
Density of material	2,667. 10^{-6}	Kg/mm^3
Poison's ratio	0.28	
Elasticity modulus	1,712	Gpa
Material constant (K)	6.762	Gpa
Strain hardening exponent	0.1	
Strain rate sensitivity index	0.5	
Initial strain rate	1. 10^{-8}	/ms
Viscoplastic	Active	

The decomposition of the deformation into elastic and plastic parts can be written as follows:

$$\dot{\varepsilon}_{ij} = \dot{\varepsilon}_{ij}{}^{el} + \dot{\varepsilon}_{ij}{}^{pl} \tag{5}$$

The Cauchy stress tensor can be decomposed into deviatoric and hydrostatic part.

$$\sigma_{ij} = S_{ij} + \sigma_H I \tag{6}$$

The deviatoric part can be obtained from:

$$S_{ij} = 2\mu_e \dot{\varepsilon}_{ij}{}^{pl} \tag{7}$$

The hydrostatic part can be determined through:

$$\sigma_H = \lambda_e \dot{\varepsilon}_{kk}{}^{el} \delta_{ij} \tag{8}$$

Where μ_e and λ_e are the Lamé constants.

$\dot{e}_{ij}{}^{pl}$ is the deviatoric plastic strain tensor, which can be obtained as :

$$\dot{e}_{ij}{}^{pl} = \dot{\varepsilon}_{ij} - \frac{1}{3}\dot{\varepsilon}_{kk}\delta_{ij} \tag{9}$$

The viscosity μ is then obtained from the expression below :

$$\mu = \frac{1}{3}K\dot{\varepsilon}_{eq}{}^{m-1} \tag{10}$$

To ensure that reasonable results could be obtained by using the creep model, a simulation was carried out to model a uniaxial tensile test. The material constants obtained from tensile test were applied in the constitutive equation and similar conditions such as constant strain rate, geometry of the specimen, clamping of the specimen were included.

The exponential velocity profile demonstrated in equation (2) was used as a boundary condition to constrain the displacement of the nodes in the clamped area. Verification was conducted by comparing the results from finite element and from the tensile test.

A good agreement was obtained in the steady state condition (see Fig. 5). Finite element model assumed that the constitutive model as function of strain rate. Therefore, as long as strain rate was constant, the condition was steady state. It meant that the strain have no role in increasing the stress. On the contrary, the strain hardening and plastic instability occurred in the tensile tests. As superplasticity stipulated homogenous micro grains, as matter of fact, grain growth could not be avoided due to exposing in recrystallisation temperature. Tensile test results indicated the occurrence of sigmoidal curve but finite element analysis came out with a linear relationship log σ and log ε.
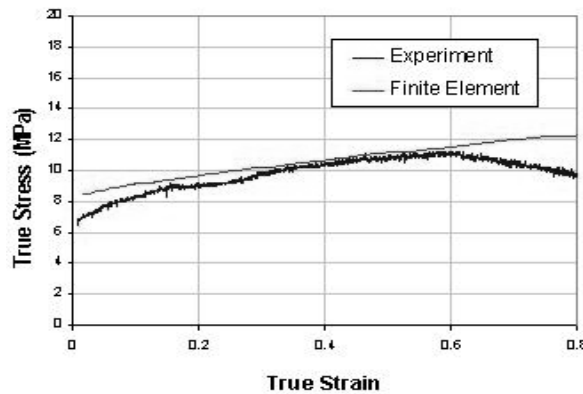

Fig. 5. Plot true stress – true strain from finite element analysis
and from uniaxial tensile test

4 The Solution Procedures of the Global Equation

In finite element analysis, there are two solution procedures of the global equilibrium equation which are adequate for metal forming, those are dynamic explicit and static implicit. Implicit method solves the equilibrium equation at the time t + which is expressed below:

$$K^T(u^{i-1})\delta u^i = F - R(u^{i-1}) \tag{11}$$

$$\Delta u^i = \Delta u^{i-1} + \delta u^i \tag{12}$$

$K^T(u^{i-1})$ is the tangent stiffness matrix of deformation system, Δu is the incremental displacement, F is the applied external load and R is the internal load vectors. Due to the non linear nature of metal forming, an iteration procedure is used to ensure that the solutions of the equilibrium equation above will satisfy the convergence criterions at each incremental step. Each iteration requires the formation and solution of the linear matrix system. With the increase of the size of problems, the matrix can be very large and very time consuming in the calculation process with computer.

Meanwhile the explicit method solves the global equilibrium equation by direct time integration:

$$\frac{M\Delta u^{t+\Delta t}}{\Delta t^2} = F^t - R^t + \frac{M\Delta u^t}{\Delta t^2} - Cv^t \tag{13}$$

$$\Delta u^t = u^t - u^{t-\Delta t} \tag{14}$$

M is the mass matrix, C is the damping matrix and Δt is the time step for time integration which is constant during the analysis. Since longer calculation time is necessary for superplastic forming where natural time is quite large, the calculation time can be reduced by increasing the mass density artificially. Higher mass density will enable us to use larger time step. As a result the analysis will complete in fewer incremental steps. However increasing the mass density will create higher inertia effect which affect the accuracy of the solution. Beside of calculation time efficiency, dynamic explicit uses a simpler algorithm to treat the contact constraints due to the small time increment.

5   Simulation of Bulge Forming of a Cup

5.1   Process Overview

Free Bulging of sheet metal is the simplest superplastic forming process. In this process, a sheet metal is clamped tightly around its periphery and a gas pressure is imposed on the surface of a sheet metal. Argon is the most favourable because its nobility. Because of the pressure, the sheet will be deformed into a die. Detail about this process could be seen in Fig. 6.

In the initial stage of deformation, the sheet is not in contact with the die. Deformation in this stage is concentrated at the pole of the dome. Consequently, greatest strain occurs in this region in this stage.
Once the pole comes into contact with the surface of the die, the material is locked against the tool by friction. This will prevent further deformation. The remaining free regions continue to deform until contact with the die occurs. Since the corner of the die usually the last to be filled, the greatest strain is occurs. As the consequent, these regions have the greatest change to suffer failure.
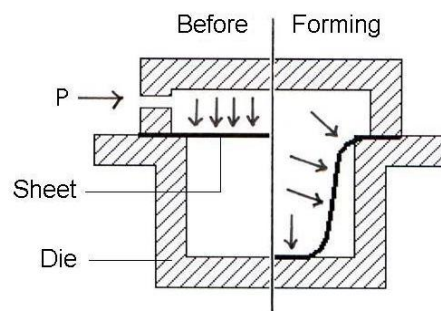

Fig. 6. Free bulging

Some idealisations and simplifications of physical and mechanical phenomena have been made to ease the finite element analysis, they were as follows :

1. It was assumed that no material flow occurs at the periphery because the sheet was clamped tightly at this area.
2. The process took place in an isothermal condition, therefore, gradient temperature between the sheet metal, die and blowing gas or fluid did not occur. In this analysis, superplastic forming was carried out at temperature 510 ^{o}C.
3. Because of equiaxed grains of superplastic materials due to termo-mechanical heat treatment, it was assumed that the superplastic material had isotropy properties.
4. There was no effect of grain growth during the process, therefore the flow curve depended only on the mechanical characteristics.
5. Friction condition due to lubrication with Boron Nitride was assumed as glide friction.

5.2　Discretisation and Boundary Conditions

The 1.6 mm sheet was divided into elements defined as shell elements. Belitschko-Tsay model with 3 integration points has been chosen for the sheet. The die was defined as a rigid body and the elements of the die were very thin. Radial meshing technique was required due to the stress system working in this axisymmetric model. The circlemesh technique has been used in this analysis.
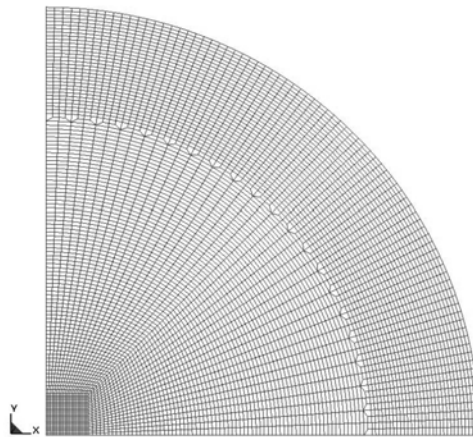
Fig. 7. Discretization of the blank with circlemesh

In this analysis, the adaptive meshing was not able to be activated. Considering the large deformation of the elements, adaptivity would be very useful, especially to simulate a complicated geometry. A smooth contour could be produced if adaptivite meshing was enabled. The most possible solution for this problem was to generate a very fine mesh, but using very fine mesh would consume more cpu time. However it is indeed not sufficient to follow a complex contour.

Due to simplification above, boundary conditions could be imposed in the system easily. In order to shorten the calculation time, the analysis for this bulge forming has been carried out only for a quarter of the cup by using symmetry constrains. Pressure was applied on the surface of the sheet and the positive normal Z direction of the pressure was opposite to the normal direction of the sheet.

5.3 Mass scaling & Contact Definition

The mass scaling has been applied in order to accelerate the calculation time, as well as to enable the calculation to be carried out in real time. Due to the very fine mesh, analysis without mass scaling will take unreasonable cpu time.

A contact between the sheet and the die was defined as CONTACT_CONSTRAINT_NODES_ TO_SURFACE. This contact option has been chosen because the penalty method was not reliable if mass scaling was applied. The analysis will be automatically terminated if a given amount of nodes has been in contact with the surface of the die. The surface of the sheet metal that moves toward the die was defined as slave segment and the surface of the die was defined as master segment.

5.4 Pressure Control Algorithm

The main objective of the superplastic analysis is to predict the pressure time history, in which the strain rate is maintained low and constant in correspond with the highest m value. For this purpose, pressure control algorithm has to be developed. High m value indicates the high resistance of necking, therefore an exceptional elongation can be reached.

5.4.1 Algorithm from LS-DYNA

To control the strain rate, LS-DYNA calculates the ratio between the expected optimal strain rate and the maximum strain rate of the model:

$$R = \frac{\dot{\varepsilon}_{op}}{\dot{\varepsilon}_{\max}} \tag{15}$$

If R is less than 1, the pressure must be decreased, and if R is greater then 1, the pressure must be increased. During the numerical simulation, the pressure can be adjusted using a pressure multiplier p_{mult} and the new pressure is obtained through:

$$p_{new} = p_{old} \, p_{mult} \tag{16}$$

Where p_{new} is the new pressure prediction at the start of a new calculation step, p_{old} is the pressure from the previous step. p_{mult} is determined as a function of the strain rate ratio R.

$$P_{mult} = f(R) \tag{17}$$

At the start of numerical simulation, the pressure multiplier is chosen to be 1. During the first several steps, the pressure can be aggressively increased until R approaches 1.0 using equation below :

$$p_{new} = p_{old} R^n \tag{18}$$

The parameter n can be chosen to be equal to the strain rate sensitivity m. After several step, when R is about equal to 1, n should be decreased to avoid a large increase in the pressure multiplier. If the starting pressure from equation (18) is too high and R is less than 1 for one or more step, the pressure can be cut back using a formulation below:

$$p_{new} = p_{old} + \frac{(p_{new} - p_{old})}{w} \tag{19}$$

The cut back parameter w is chosen to be greater than 1.0 or 1.2.

5.4.2 Algorithm from ABAQUS

The formulation of pressure control algorithm is implemented by means of solution dependent amplitude. The applied pressure p is to be varied throughout the simulation to maintain the current strain rate $\dot{\varepsilon}$ at an optimal predetermined value $\dot{\varepsilon}_{op}$. Mathematically, this constrain is written as :

$$g = \dot{\varepsilon} - \dot{\varepsilon}_{op} = 0 \tag{20}$$

The objective here is to determine the displacement u^t and the applied external pressure p^t that satisfy the global equilibrium equation from finite element discretization in which external forces from the applied load is equal to internal forces from stresses in corresponding with displacements.

$$F(p^t) = R(u^t) \tag{21}$$

As well as external constraint:

$$g(u^t) = 0 \tag{22}$$

Since the solution of the global equation is performed on an incremental form. The discrete analogue of the equation above is to find u^{n+1} and p^{n+1}, so that:

$$F(p^{n+1}) = R(u^{n+1}) \tag{23}$$

$$g(u^{n+1}) = 0 \tag{24}$$

Where n is the increment number. ABAQUS calculates the value of γ_{max} which expresses the ratio of the maximum equivalent strain rate to the optimal predetermined strain rate for any integration point in a specified element set.

$$\gamma_{max} = \frac{\dot{\varepsilon}_{max}}{\dot{\varepsilon}_{op}} \tag{25}$$

Assumed that all quantities are known at increment n, pressure control algorithm is developed as follows [11]:

|		
If $\gamma_{max} < 0.2$,	then $p_{r+1} = 2.0\ p_r$	(26)
If $0.2 < \gamma_{max} < 0.5$,	then $p_{r+1} = 1.5\ p_r$	(27)
If $0.5 < \gamma_{max} < 0.8$,	then $p_{r+1} = 1.2\ p_r$	(28)
If $0.8 < \gamma_{max} < 1.5$,	then $p_{r+1} = 1.0\ p_r$	(29)
If $1.5 < \gamma_{max} < 3.0$,	then $p_{r+1} = 0.5\ p_r$	(30)
If $\gamma_{max} > 3.0$,	then $p_{r+1} = 0.5\ p_r$	(31)

Where p_{r+1} is the new pressure value corresponding to the iteration r+1 and p_r is the old pressure value corresponding to the iteration r. This algorithm is not proposed to follow the target strain rate exactly but to obtain a practical pressure time history.


5.5   Results and Discussion

5.5.1 Pressure Cycle

In general, finite element has generated a similar tendency to other non-finite element analysis, which was called top hat pattern shown in Fig. 8a. The pressure reached a maximum value at a point and hereafter the pressure lowered to the minimum point. At the first stage, the pressure increased gradually with the time, from 0 until a maximum value was reached. After that, the pressure decreases gradually until contact occurs. At the second stage, the sheet came in contact with the die, and the pressure rose sharply to overcome the friction which occurred between surfaces. The results of finite element can be seen in Fig. 8b.

LS-DYNA produced higher pressure than ABAQUS. It was a consequence of the pressure algorithm, in which the pressure could be increased aggressively by using exponential relationship expressed in equation (18). But If the pressure created a very high strain rate, the new pressure could not be decreased sharply but gradually using equation (19). Beside of that, the pressure would be cut back by a minimum pressure multiplier if buckling occurred.
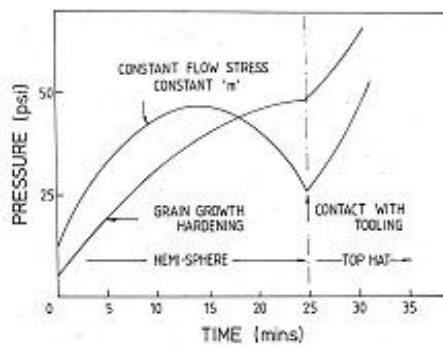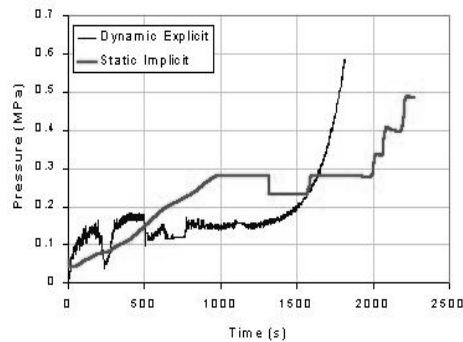
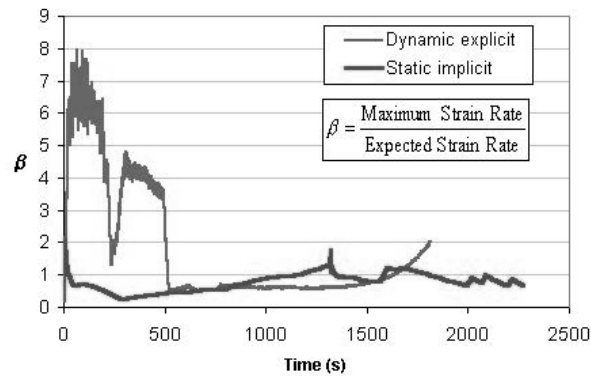| a. Non-FEM [12]	b. FEM; dynamic explicit and static implicit for expected strain rate 1.10^{-3}/s

Fig. 8. Pressure-time cycle

LS-DYNA calculated the pressure in a certain range. The range was determined by using a maximum and minimum multiplier, so that the pressure would not exceed a reasonable value. A very low value of minimum multiplier would generate a very low pressure if buckling occurs. Consequently, after buckling, the deformation would not go further continue until the pressure was high enough. In this algorithm, the first pressure value had to be predicted closely. Simplified quantitative analysis (non FEM) such as Dutta-Mukherjee [13] could be used.

In the first stage before the contact. The both LS-DYNA came out with maximum pressure about 0.2 Mpa and ABAQUS 0.3 Mpa. In the second stage, after contact occurred, LS-DYNA increased the pressure more sharply than ABAQUS. Consequently, the process ended faster.

5.5.2 Strain Rate Profile

To ensure that the strain rate did not exceed the targeted strain rate, the principle strain rates of all elements were calculated and the maximum strain rate values are written. An expression β indicates the ration between maximum strain rate and the expected strain rate. Fig. 9 demonstrated the strain rate profile. Considering the results from tensile tests, which determined that allowed strain rate is 1.10^{-2}/s or maximum β value 10, the both results from dynamic explicit and implicit are in the superplastic range. But, ABAQUS was able to maintain the strain rate in a more narrow range than LS-DYNA. Maximum ratio of strain rate was reached is 1.9, while LS-DYNA reached 7.95.

Fig. 9. Strain rate history from dynamic explicit and static implicit
for expected strain rate 1.10^{-3}/s

5.5.3 Height and Thickness of the Dome

Comparing the height of the dome from ABAQUS and LS-DYNA. For both analyses, the times in which the contact occur were close. In ABAQUS, the contact came at 1290 sec and at 1200 sec in LS-DYNA. The height and thickness of the dome from the cup test can be seen in Fig. 10.

In other simulations, the friction condition was defined to be sticking friction in which coefficient of friction was set to be 1 [14, 15], therefore there will be no further movement of the nodes after contact occurs. However, in this simulation, the value of friction coefficient was set to be 0,3 or sliding friction. Consequently, thickness reduction carried on after the sheet was in contact with the die.
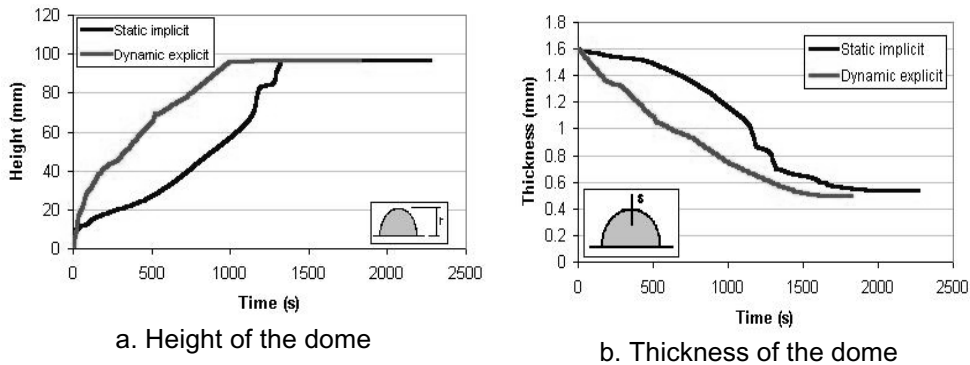

a. Height of the dome

b. Thickness of the dome

Fig. 10. Height and thickness of the dome from dynamic explicit and static implicit

5.5.4 Thickness Distribution

The thickness distribution can be seen in Fig. 15. As mentioned before, the thinnest area was the area that was the latest in contact with the die. Thickness distributions in both ABAQUS and LS-DYNA were nearly similar.
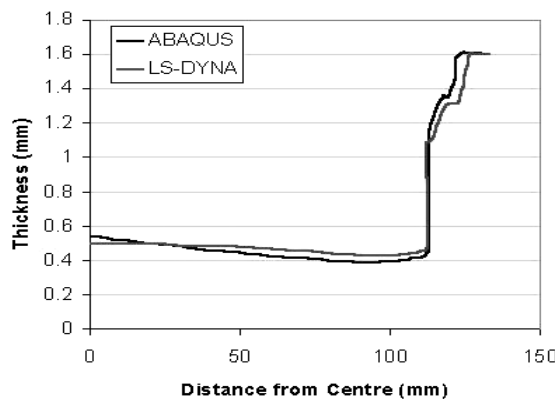

Fig. 11. Thickness Distribution of the cup from dynamic explicit and static implicit

5.5.5 The Effects of Strain Rate Sensitivity Index (m) and Friction Coefficient

In this analysis, m was varied to see its influence to the resistance of thinning. The forming process was terminated at the first stage of bulge forming, in order to see the differences more clearly without the influence of friction factor.
The original m value from tensile test data was 0.5 and comparison was made for m value 0.5, 0.65 and 0.75. Figure 16 shows the results.

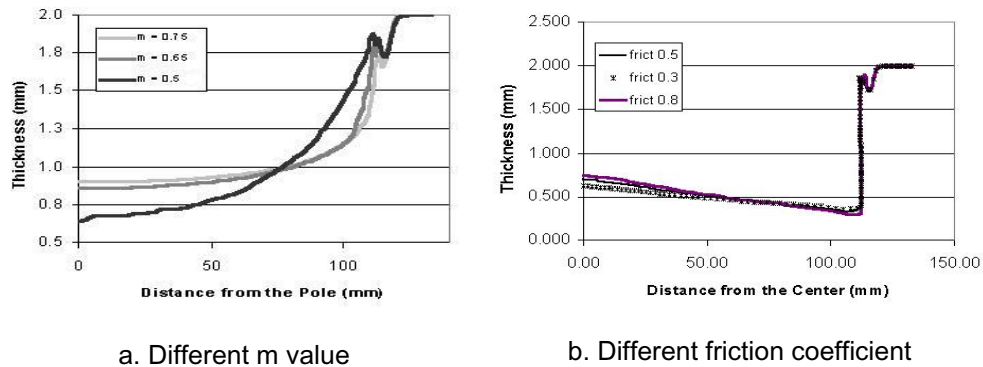a. Different m value   b. Different friction coefficient

Fig. 12. Thickness distribution for different variables

As known, the m value describes the property of the material against thinning or necking. The higher the m value, the better the thinning resistance and the more homogeneous thickness would be produced. At the pole, the highest m value 0.75 produced highest thickness 0.904 mm. Increasing the m value improved the distribution significantly. One of the ways to increase the m value was by increasing the process temperature.

Three values of friction coefficients have been applied to understand the influence of friction to the thickness distribution. The coefficient values were: 0,3, 0.5 and 0.8. It is shown that there was only a slight distinction. In the centre of the cup, the biggest thickness difference occurred. In the wall and in the corners, the thickness was nearly similar for the three friction coefficients.

6   Conclusion

Creep constitutive equation could be applied to model superplastic behaviour of Aluminium alloy 5083. However, the material parameters should be determined carefully. Tensile tests of constant strain rates were carried out and they came out with good results. The strain rate could be maintained constant during uniaxial tensile test by changing the crosshead velocity continuously according to exponential relationship between velocity and time. It is demonstrated that the expected value of the true strain could be approached very well. The maximum m value for Aluminium alloy 5083 at $510^{o}C$ was 0.5 in the range strain rate 1.10^{-4} – 1.10^{-2} /s.

As superplastic deformation stipulated a narrow range of strain rates, the gas pressure had to be controlled. For this purposes algorithms of pressure control were developed. LS-DYNA and ABAQUS were able to show right tendencies in modelling superplastic behaviour. The "top hat" pattern of pressure-time cycle has been generated. ABAQUS had a simpler algorithm from LS-DYNA. Using LS-DYNA, the pressure input should be predicted more carefully. As implicit procedure establishes the global equilibrium equation and solves the equation with a more correct physically approach, implicit came out with better results. However, dynamic explicit procedure was more time efficient. Considering the thickness distribution, the results from LS-DYNA and ABAQUS differed insignificantly.

LS-DYNA was able to model the effect of strain rate sensitivity index m. Three different values of m have been applied and the results from finite element analysis have shown that m affected the thickness distribution significantly. The value of friction coefficient have been varied and the results indicated that thickness distribution was not affected significantly by friction condition.

References

1. Higashi K et al., "An experimental investigation of the superplastic forming behavior of a commercial Al-bronze", *Metallurgical Transaction* 1990; 21A(11): 2957-2966.
2. *SUPERFORM Brochure: a Design Manual and Source Book for Aerospace Engineers and Designers*
3. Jovane F, An Approximate Analysis of the Superplastic Forming of a Thin Circular Diaphragm: Theory & Experiments*, International Journal of Mechanical Science* 1968; 10: 403-427
4. Holt DL., An Analysis of the Bulging of Superplastic Sheet by lateral Pressure, *International Journal of Mechanical Science* 1970; 12: 491-197.
5. Ragab AR, Thermoforming of Superplastic Sheet in Shaped Dies, *Metals Technology* 1983; 10: 340-348.
6. Chandra N, Kannan D, Superplastic Sheet metal Forming of a Generalised Cup, Part 1 : Uniform Thinning, *Journal of Materials Engineering and Performance* 1992; 1(6): 801-811.
7. Padmanabhan KA, Vasin RA, Enikeev FU. *Superplastic Flow: Phenomelogy and Mechanics,* Springer Verlag, Berlin 2001: 11.
8. Backofen WA, Turner IR, Avery DH. Superplasticity in an Al-Zn Alloy. *Transaction of American Society for Metals* 1964; 57: 980-990.
9. Suery M, Baudelet B. Theoretical and Experimental Constitutive Equation of Superplastic Behaviour: Discussion. *Journal of Materials Science* 1975; 10(6): 1022-1028.
10. Verma R, et al. Characterisation of Superplastic Deformation Behaviour of a Fine Grain 5083 Al Alloy Sheet. *Metallurgical and Material Transaction A* 1996; 27A(7): 1889-1898.
11. *ABAQUS Standard User's Manual Version 6.2*, Volume 2, Hibbit, Karlsson & Sorensen Inc, USA, 2001
12. Pilling J, Ridley N. *Superplasticity in Chrystalline Solid*, Institute of Metals, London 1989: 175.
13. Dutta A, Mukherjee AK, *Superplastic Froming : An Analytical Approach,* Material Science and Engineering, 1992; A157: 9-13.
14. Hu P, et al, "Rigid Viscoplastic Finite Element Analysis of the Gas Pressure Constrined Bulging of Superplastic Circular Sheets into Cone Disk Shape Dies", *International Journal of Mechanical Science,* 1997; 39(4): 487-496.
15. Nakamichi S, et al, "A Numerical Analysis of the Hydrolic Bulging of Circular Disks into Axysymmetric Dies", *Journal of Applied Mechanics*, 1982; 42.
16. *LS-DYNA Keywords Users Manual version 960*, Livermore Software Technology Corporation, 2001